

Heme Oxygenase-1 (HO-1) Induces Resistance to Ferroptosis in Gastric Cancer by Targeting GPX4

Shiqi Shi^{1#}, Hanyu Wang^{1,2#}, Xiaolu Yu³, Huiyao Li^{1,2#}, Shuai Liang⁵, Dong Hua^{1,2,5*}

ABSTRACT

Gastric cancer, a prevalent gastrointestinal tumor, experiences limited efficacy with conventional surgery and chemotherapy. Hence, the imperative to identify additional therapeutic targets is underscored. Numerous studies have reported heme oxygenase-1 (HO-1) for its antioxidant and protective attributes on organs and tissues. In the present study, the role of HO-1 in stimulating the proliferation of gastric cancer cells was explored. The hypothesis posited that HO-1 facilitates gastric cancer progression by regulating GPX4 and ferroptosis. Analysis through bioassay and immunohistochemistry revealed a significant augmentation in HO-1 expression within gastric cancer tissues. Mechanistically, real-time fluorescence quantitative PCR and protein immunoblotting confirmed that HO-1 modulates the protein expression of GPX4, a pivotal player in ferroptosis regulation. Through the upregulation of mRNA expression for GPX4, HO-1 inhibits ferroptosis, thereby fostering gastric cancer progression. This is achieved by elevating GPX4 protein levels and diminishing intracellular reactive oxygen species in gastric cancer cells. In summary, our results elucidate the protective role of high HO-1 expression against ferroptosis in gastric cancer cells, thereby promoting their malignant progression. The upsurge in HO-1 expression emerges as a potential tumor marker and therapeutic target for gastric cancer, offering a novel avenue for intervention.

INTRODUCTION

Gastric cancer persists as a significant global malignancy of the digestive tract, ranking fifth in incidence and fourth in mortality worldwide Sung et al. (2021). The high proliferative capacity of gastric cancer cells poses a substantial challenge; however, the underlying mechanisms of cancer cell proliferation are unclear. The unfavorable prognosis for patients with gastric cancer predominantly stems from inadequate responses to current treatments Cristescu et al. (2015). Therefore, it is imperative to identify precise and novel treatment modalities for patients with gastric cancer.

Ferroptosis, a form of cell death distinct from apoptosis, necrosis, and autophagy characterized by iron-dependent accumulation of reactive oxygen species (ROS) leading to lipid peroxidation, has emerged as a noteworthy phenomenon Dixon et al. (2012). Numerous genes and proteins implicated in regulating iron metabolism play pivotal roles in ferroptosis Alam et al. (2007), Frazer et al. (2014), Bogdan et al. (2016), Gao et al. (2015). In recent years, the role of ferroptosis in gastric cancer has revealed protective mechanisms, such as Wnt/beta-catenin signaling Sun et al. (2015) and cancer-associated

fibroblasts Wang et al. (2022), which shield gastric cancer cells from ferroptosis, thereby advancing the progression of gastric cancer.

GPX4 is known to be a lipid repair enzyme that plays a key role in the regulation of ferroptosis Dixon et al. (2012). Accumulating evidence suggests that GPX4 is regulated on the activity and stability level Song et al. (2020), Dang et al. (2022), Li et al. (2023). For example, there are studies that show both Nrf2 and HO-1 could be inducible and participate in the synthesis of GPX4 Song et al. (2020). At the same time, the activation of Nrf2/HO-1/GPX4 pathway significantly ameliorated the oxidative stress injury of mouse neurons Dang et al. (2022). A related team has also observed that CSTI improves the stability of GPX4 protein by inhibiting the ubiquitin-protease system (UPS) Li et al. (2023). However, the role of GPX4-ferroptosis in gastric cancer remains unclear.

Molecularly targeted therapy, a novel approach to treating malignant tumors, has gained prominence in recent years. Heme oxygenase-1 (HO-1), the rate-limiting enzyme in heme catabolism, has three identified mammalian subtypes, such as HO-1, HO-2, and HO-3.

¹Wuxi school of medicine, Jiangnan university

²The Affiliated Children's Hospital of Jiangnan University

³The Second People's Hospital of Jingdezhen

⁴Department of Oncology, The Affiliated Wuxi People's Hospital of Nanjing Medical University, WuXi Medical Center, WuXi, China.

Correspondence to: Dong Hua, Department of Oncology, The Affiliated Wuxi People's Hospital of Nanjing Medical University, No. 299, Qingyang Road, Wuxi, 214000, Jiangsu, P. R. China; Email: 421459855@qq.com.

Key words: Gastric cancer, HO-1, Ferroptosis, GPX4.

HO-1 and HO-2 are present in humans and rats, while HO-3 is found exclusively in rats. The HMOX2 subtype is constitutively expressed, encoding a 36 kDa HO-2 protein that primarily maintains the basal metabolism of heme. Moreover, HO-1 is inducible, and its synthesis is enhanced in response to prooxidative stimuli, encompassing oxidants, cytokines, heavy metals, and physical cues such as ischemia/reperfusion injury and hypoxia/hyperoxia. Encoded by the HMOX1 type, HO-1 has an approximate molecular weight of 32 kDa, also recognized as heat shock protein Kwon et al. (2015).

HO-1 catalyzes heme degradation, yielding carbon monoxide, ferrous iron, and biliverdin. Notably, chlorophyll exerts a protective effect by inhibiting lipid and protein peroxidation through the scavenging of ROS Hassannia et al. (2018). HO-1 acts as a dual regulator of iron and ROS homeostasis Zhang et al. (2020), Ryter et al. (2006) and is deemed to exert a prominent influence in the context of iron-induced cell death Vitek et al. (2007), Kwon et al. (2015), Chang et al. (2018). Moreover, a correlation was observed between increased HO-1 expression and heightened lipid peroxidation in patients with Alzheimer's disease Sugimoto et al. (2012). In addition, upregulation of HO-1 has demonstrated efficacy in preventing hepatic fibrosis caused by peroxidation Deshane et al. (2017). HO-1-mediated ferroptosis emerges as an essential factor in the retinal pigment epithelial cell degeneration Luo et al. (2022).

However, a deeper investigation into the role of HO-1 reveals contradictory evidence, suggesting that HO-1 may accelerate tumor progression. For instance, high HO-1 expression in a mouse model of human primary head and neck squamous carcinoma correlated with faster malignant progression Jomova et al. (2010). HO-1 overexpression in pancreatic cancer cells significantly promoted tumor angiogenesis and accelerated lung metastasis development Sunamura et al. (2003). Despite these findings, the molecular mechanisms by which HO-1 promotes malignant progression in gastric cancer require further exploration.

In the present study, we investigated the role of HO-1 in promoting gastric cancer, positing a hypothesis that HO-1 could potentially inhibit gastric cancer progression by regulating GPX4 and ferroptosis.

MATERIALS AND METHODS

Cell lines and cell culture

Human gastric cancer cell lines AGS and HGC-27 were procured from Wuhan Procell Life Science & Technology Co, and MKN-45, NCL-N87, and GES-1 were obtained from iCell Bioscience Inc, Shanghai. These cell lines were confirmed to be free of mycoplasma contamination. All cell lines were cultured in RPMI 1640

(Gibco, Thermo Fisher Scientific, Germany) supplemented with 10% fetal bovine serum (Meisen CTCC) and 5% penicillin and streptomycin. The cells were maintained in a humidified atmosphere with 5% CO₂ at 37°C and used during their logarithmic growth phase.

Tissue specimens

Primary GC tissues and corresponding noncancerous paracancerous tissues were collected from 30 patients with gastrectomy who underwent gastrectomy without neoadjuvant therapy at Wuxi People's Hospital from 2018 to 2023.

Quantitative real-time PCR (RT-qPCR)

Total RNA was isolated from cultured cells using the standard Trizol (Invitrogen) protocol. Its integrity, quantity, and purity were assessed using a NanoDrop 2000c spectrophotometer (Thermo Fisher Scientific, Wilmington, USA). Subsequently, 1 µg of total RNA was reverse transcribed using an all-in-one 5 × RT MasterMix (ABM, Canada). Real-time fluorescence quantitative PCR reactions were performed on an ABI ViiA7 Sequence Detection System (Life Technologies, USA) using SYBR Green Premix (ABI). Relative gene expression levels were analyzed using the comparative Ct method, where Ct is the cycle threshold number normalized to GAPDH. The primer sequences for HO-1 and GPX4 are provided below.

HO-1: Forward: 5'-GGCCTCCCTGTACCACATCT-3',

Reverse: 5'-CTGCATGGCTGGTGTGTAGG-3'.

GPX4:

Forward: 5'-ACGTCAAATTCGATATGTTTCAGC-3',

Reverse: 5'-AAGTTCCACTTGATGGCATTTC-3'.

Western blot

Cell lysates were prepared by combining protease and phosphatase inhibitors in equal proportions with radioimmunoprecipitation assay buffer. The protein concentration was quantified using the BCA Protein Assay kit (Yeasen Biotechnology, Shanghai). A total of 20 µg of proteins were separated using SDS-PAGE and electroblotted onto a PVDF membrane. The membrane was then enclosed in TBST containing 5% skim milk powder for 1 h and incubated with primary antibodies at 4°C overnight. After washing thrice with TBST for 10 min each, the membrane was incubated with secondary antibodies diluted in a blocking buffer for 1 h at room temperature. Subsequently, the samples were rewashed three times with TBST and subjected to enhanced chemiluminescence (ECL) using an ECL kit (Yeasen Biotechnology, Shanghai). Densitometric analysis was

conducted using ImageJ software.

Antibodies for HO-1 (rabbit monoclonal antibody, abs159446, 1:1000), GPX4 (rabbit monoclonal antibody, abs136221, 1:1000), and β -Actin (rabbit monoclonal antibody, abs132001, 1:10,000) were procured from Shanghai Univision Co. GAPDH (murine monoclonal antibody, Cat No. 60004-1-Ig, 1:10,000) was obtained from Proteintech (Wuhan, China).

CCK8 assay

The CCK8 assay was performed following the manufacturer's manual (Taojiao Biotechnology, Shanghai, China). In brief, 10,000 cells in 100 μ l of culture were added to each well of a 96-well plate for 24, 48, and 72 h. At each time point, 10 μ l of sterile CCK-8 was added to each well, and after 1 h of incubation at 37°C, the absorbance was measured at 450 nm using an enzyme meter.

Small interfering RNAs (siRNAs), overexpression plasmids, and transfection protocol

All siRNAs and plasmids for HO-1 overexpression were obtained from Suzhou Gemma Genetics Co. Cell transfection was performed following the Lipofectamine 3000 (Thermo Fisher Scientific, Germany) manual. RT-qPCR and protein blotting were used to detect the plasmid-mediated overexpression and silencing efficiency of HO-1 in GC cells. The sequences for siRNA and overexpression vectors are listed below.

siRNA:

HMOX1-Homo-263:

sense(5'3')CCCUGUACCACAUCUAUGUTT;

antisense (5-3')ACAUAGAUGUGGUACAGGGTT.

HMOX1-Homo-196:

sense(5'3')GCUGAGUUCAUGAGGAACUTT;

antisense(5'-3')AGUUCCUCAUGAACUCAGCTT

Conventional overexpression vectors:

HMOX1 Home:

(5'3')

ATGGAGCGTCCGCAACCCGACAGCATGCCCA
GGATTTGTCAGAGGCCCTGAAGGAGGCCACC
AAGGAGG

TGCACACCCAGGCAGAGAATGCTGAGTTCAT
GAGGAACITTCAGAAGGGCCAGGTGACCCGA
GACGGCTT

CAAGCTGGTGATGGCCTCCCTGTACCACATCT
ATGTGGCCCTGGAGGAGGAGATTGAGCGCAA
CAAGGAG

AGCCCAGTCTTCGCCCCGTGTCTACTTCCCAGA
AGAGCTGCACCGCAAGGCTGCCCTGGAGCA
GGACCTGG

CCTTCTGGTACGGGCCCCGCTGGCAGGAGGT
CATCCCCTACACACCAGCCATGCAGCGCTATG
TGAAGCG

GCTCCACGAGGTGGGGCGCACAGAGCCCGA
GCTGCTGGTGGCCACGCCTACACCCGCTAC
CTGGGTGAC

CTGTCTGGGGGCCAGGTGCTCAAAAAGATTG
CCCAGAAAGCCCTGGACCTGCCAGCTCTGG
CGAGGGCC

TGGCCTTCTTCACCTTCCCCAACATTGCCAGT
GCCACCAAGTTCAAGCAGCTCTACCGCTCCCG
CATGAA

CTCCCTGGAGATGACTCCCGCAGTCAGGCAG
AGGGTGATAGAAGAGGCCAAGACTGCGTTC
CTGCTCAAC

ATCCAGCTCTTTGAGGAGTTGCAGGAGCTGC
TGACCCATGACACCAAGGACCAGAGCCCCTC
ACGGGCAC

CAGGGCTTCGCCAGCGGGCCAGCAACAAAGT
GCAAGATTCTGCCCCCGTGGAGACTCCCAGA
GGGAAGCC

CCCCTCAACACCCGCTCCAGGCTCCGCTTC
TCCGATGGGTCCITACACTCAGCTTTCTGGT
GGCGACA

GTTGCTGTAGGGCTTTATGCCATGTGA

Measurement of lipid peroxidation

Total cellular lipid peroxidation was measured using the C11 BODIPY (581/591) probe (Thermo Fisher Scientific, Germany). Cells were treated as indicated and incubated with 10 μ M of C11 BODIPY in fresh medium for 30 min at 37°C. Subsequently, excess C11 BODIPY was eliminated by washing the cells twice with PBS. The labeled cells were trypsin-digested, resuspended in PBS, and subjected to flow cytometry analysis. Oxidation of the polyunsaturated butadiene fraction of C11 BODIPY induced a shift in the fluorescence emission peak from ~590 nm to ~510 nm, correlating with lipid peroxidation production, and was evaluated using a flow cytometer (BD Biosciences, USA).

Measurement of ROS

DCFH-DA (Thermo Fisher Scientific, Germany) was used to measure ROS levels following the manufacturer's protocol. Briefly, cells were seeded in 6-well plates and exposed to Erastin for 24 h. After the

treatment, cells were harvested, washed twice with PBS, and subjected to labeling with 20 μ M DCFH-DA for 30 min at 37°C. The labeled cells were collected, and their DCF fluorescence intensity was analyzed using flow cytometry (BD Biosciences, USA).

Determination of the labile iron pool

The labile iron pool was determined using FerroOrange, an orange fluorescent probe specialized for detecting unstable iron (II) ions (Fe²⁺). Cells were seeded in 6-well plates and treated with Erastin for 24 h. After treatment, cells were washed twice with PBS and incubated with 2 μ M FerroOrange (Maokang Biotechnology Co., Ltd., Shanghai) for 30 min at 37°C. Subsequently, the cells were washed with PBS and analyzed using fluorescence microscopy. The absorption maximum was observed at 542 nm for FerroOrange, and the fluorescence maximum was observed at 572 nm. The level of unstable iron was calculated based on the average fluorescence intensity of the cells.

Measurement of glutathione

Monochlorobimane was used to detect GSH in cells. Cells were seeded in 6-well plates and treated with Erastin for 24 h. After treatment, cells were washed twice with PBS and incubated with 20 μ M monochlorobimane (mBCL, HY-101899, MedChemExpress) for 30 min at 37°C. After three washes with fresh serum-free medium, the associated fluorescence intensity was measured using flow cytometry or fluorescence inverted microscopy under specific excitation (Ex: 380 nm) and emission (Em: 470 nm) light.

Bioinformatic analysis

1.1. Ferroptosis-Related Genes Collection

A collection of ferroptosis-related genes consisting of 721-encoded proteins was obtained from the GeneCards database (<https://www.genecards.org/>).

1.2. Gene Expression Data Collection

mRNA data and clinical information for patients with stomach adenocarcinoma (STAD) were collected from The Cancer Genome Atlas (TCGA). The discovery cohort, obtained from TCGA, consisted of data on patients with STAD. A total of 18,587 differentially expressed genes were identified using the differential analysis between GBM and normal tissues.

Statistical analysis

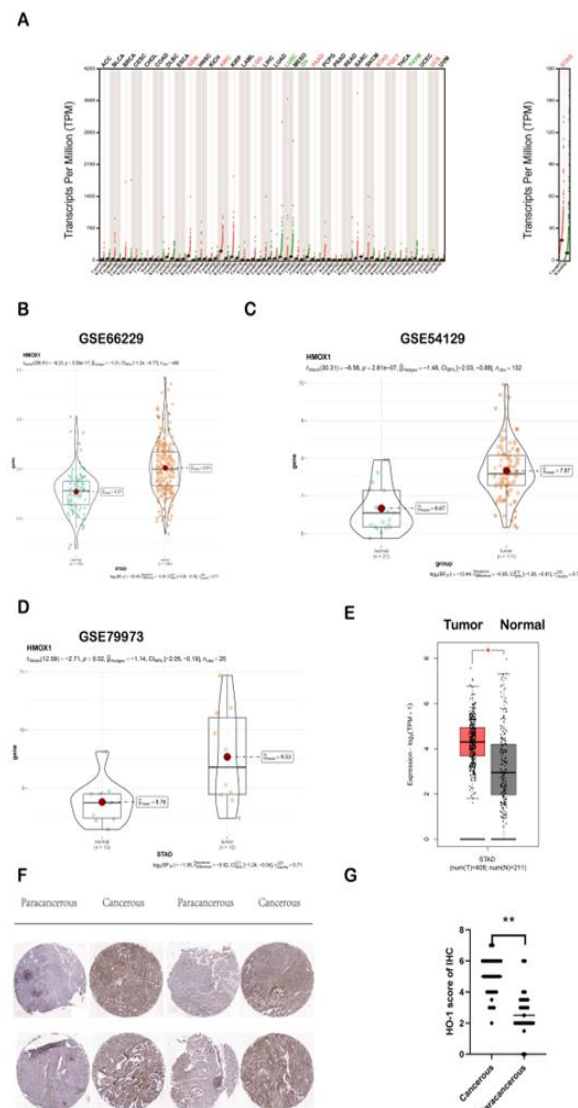
All experiments were conducted at least three times, and data are expressed as mean \pm SD. Statistical significance between treatments was assessed using Student's t-test, with p-value < 0.05 considered statistically significant.

RESULTS

Upregulation of HO-1 in primary gastric cancer

Our pan-cancer analysis using the GEPIA database revealed a consistent upregulation of HO-1 in primary gastric cancer tissues (Figure 1: A). To validate these findings, we corroborated the results with GEO RNA-seq analysis (GSE66229, GSE54129, GSE79973) (Figure 1: B, C, D) and the TCGA database (Figure 1: E). Four datasets consistently demonstrated a significant upregulation of HO-1 in primary gastric cancer tissues. At the same time, the immunohistochemical analysis result showed that the HO-1 was highly expressed in the GC tissues regardless of their differentiation grade (Figure 1: F). In addition, IHC of 24 paired GC and normal tissues revealed that HO-1 was highly expressed in GC tissues (Figure 1: G).

Figure 1: HO-1 is upregulated in primary gastric cancer.



A: Pan-cancer analysis of HO-1 protein was performed through the GEPIA public website.

B,C,D,E: Higher expression of HO-1 was found in GC samples than the matched normal tissues (based on GSE66229 GSE54129 GSE79973 and TCGA-STAD database).

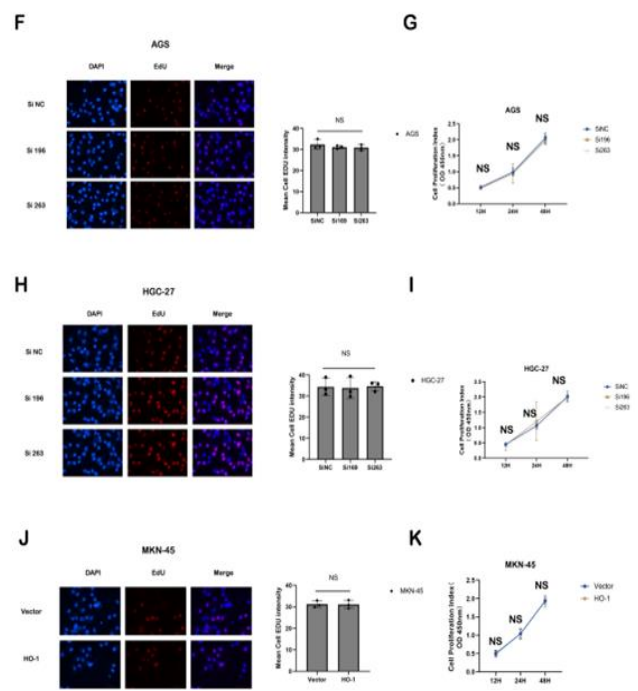
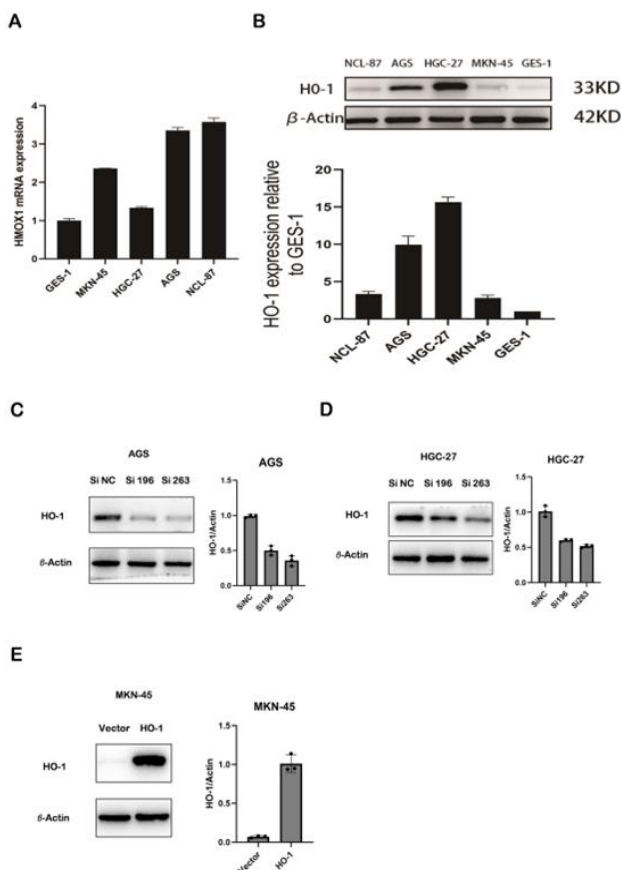
F: IHC stain scoring of HO-1 in 24 GC tissues and 24 normal tissues, statistical significance was assessed by unpaired t-test, ****<0.0001.

G:IHC stain scoring of HO-1 in 24 GC tissues and 24 normal tissues, statistical significance was assessed by unpaired t-test, ****<0.0001.

Limited impact of HO-1 on gastric cancer proliferation in vitro

Next, we examined the HO-1 mRNA and protein expression levels in GC cell lines. Examination of HO-1 mRNA and protein levels in gastric cancer cell lines revealed higher expression in AGS and HGC-27 cell lines compared to NCL-N87 and MKN-45 (Figure 2: A, B). To investigate the role of HO-1 in GC development, we performed knockdown experiments of HO-1 gene in AGS and HGC-27 cell lines with Si196 and Si263 RNA, respectively.

Figure 2: HO-1 has no effect on the proliferation of gastric cancer cells in vitro.



A, B: RT-qPCR and Western blot analysis showing the expression of HO-1 in different GC cell lines. Total β -Actin was used as a loading control.

C,D,E: Western blot analysis of AGS/HGC-27 and MKN45 transfected with HO-1 knockdown/overexpression and control. Total β -Actin was used as a loading control.

F,H,J: EDU for detection of proliferation of HGC27/AGS-siNC / HGC27/AGS-si196-HO-1 / HGC27/AGS-si263-HO-1 and MKN-45-Vector/MKN-45-HO-1 at 24 hours. Representative images (left panel) and quantification results (right panel) are shown. Data are shown as the mean \pm SD of triplicate independent sets of experiments; statistical significance was assessed by paired t-test, ns means no significance. Scale bar is: 50 μ M.

G,I,K: CCK8 assay analyzed the proliferation of MKN-45-Vector/MKN-45-HO-1 and HGC27/AGS-siNC/HGC27/AGS-si196-HO-1/HGC27/AGS-si263-HO-1 cell lines. Data are shown as the mean \pm SD of triplicate independent sets of experiments; statistical significance was assessed by paired t-test. ns means no significance.

The AGS knockdown efficiencies reached 49.50% and 35.35% (Figure 2:C), respectively, and the HGC-27 knockdown efficiencies reached 59.40% and 50.50% (Figure 2:D), respectively, indicating that we successfully reduced HO-1 expression in these two gastric cancer cell lines. In parallel, we performed overexpression experiments of HO-1 gene in MKN-45

cells (Figure 2:E) .We then used MKN-45 cells to overexpress HO-1, AGS and HGC-27 cells to knockdown HO-1 and to examine the role of HO-1 on cell behavior in vitro.CCK8 and EdU assays suggested that the overexpression of HO-1 had no effect on MKN-45 compared to control cells(Figure 2:J,K); similar results were obtained for AGS/HGC-27-si196-HO-1 and AGS/HGC-27-si263-HO-1 vs. control cells(Figure 2:F,G,H,I) .Overall, the alteration of HO-1 alone was not sufficient to inhibit the proliferation of gastric cancer cells in vitro.

Impact of HO-1 on GPX4 protein expression

To further explore the proliferative effects of HO-1 on gastric cancer cell lines, we delved into its role as a dual regulator of iron and ROS homeostasis, potentially playing a dominant role in ferroptosis Yin et al. (2012), Kwon et al. (2015), Chang et al. (2018).

So, we will explore the specific relationship between HO-1 and ferroptosis in gastric cancer. Subsequently, the TCGA-STAD genes and ferroptosis related genes was taken, and a Venn diagram was drawn.

It was found that there were 20 common genes between the two, and HO-1 was found in the intersection of these datasets, proving the existence of a certain connection between HO-1 and ferroptosis in GC (Figure 3: A). In addition,

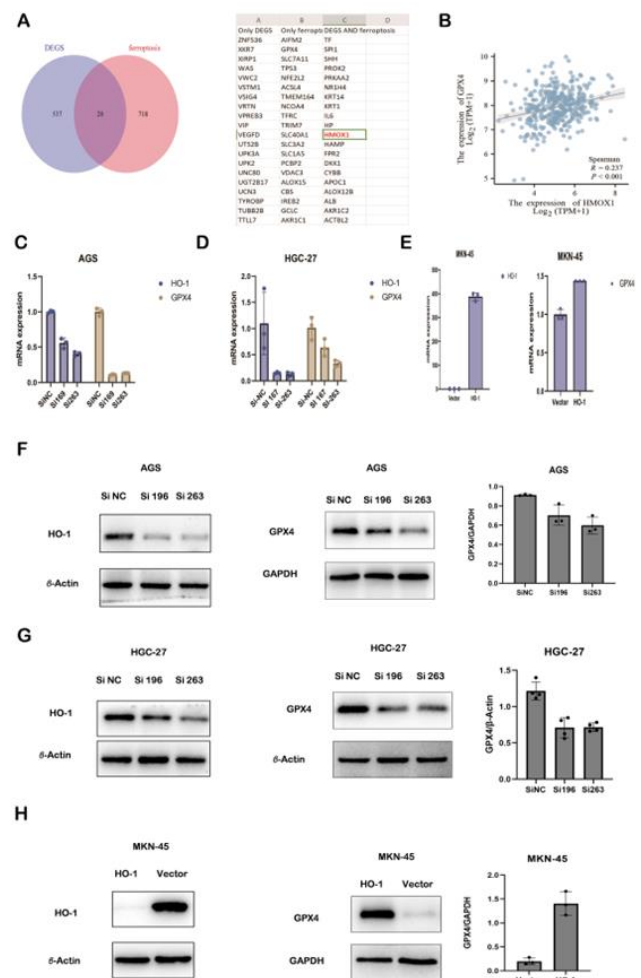
we correlated HO-1 with ferroptosis-associated proteins, and Pearson correlation line analysis in the GSE54129 dataset in the GEO database exhibited a significant correlation between HO-1 and GPX4 gene expression ($R=0.237$) (Figure 3: B).

Next, we examined the mRNA (Figure 3: C, D) and protein expression of GPX4 (Figure 3: F, G) in AGS-si196- HO-1/ AGS-si263-HO-1 and HGC-27-si196-HO-1/HGC-27-si263-HO-1 cells.

The results showed that in AGS cells, the expression of GPX4 protein and mRNA decreased by 22.99%/35.16% and 90.00%/87% in the si196/263 knockdown group cells compared to the control group; in HGC-27 cells, the expression of GPX4 protein and mRNA decreased by 46.40%/44.80% and 36.63%/66.33% in the si196/263 knockdown group cells compared to the control group. Meanwhile, we also observed in MKN-45-Vector/MKN-45-HO-1 cells that In MKN-45-HO-1 cells, the expression of GPX4 protein and mRNA was sevenfold and 1.4-fold higher than that of MKN-45-Vector, respectively(Figure 3: E, H).

In summary, these findings suggest that HO-1 positively regulates GPX4 at both the transcriptional and protein levels.

Figure 3: HO-1 affects GPX4 protein expression.



A:Gastric cancer and ferroptosis-associated genes take intersections to map Wayne diagrams.

B:Correlation analysis between HO-1 expression levels and GPX4 expression levels in the TCGA database($R=0.237$).

C,D,E: RT-QPCR showing mRNA expression of GPX4 in AGS and HGC-27 after knockdown of HO-1 and in MKN-45 after overexpression of HO-1.Data are shown as the mean \pm SD of triplicate independent sets of experiments.

F,G,I: WB showing protein expression of GPX4 in AGS and HGC-27 after knockdown of HO-1 and in MKN-45 after overexpression of HO-1.Data are shown as the mean \pm SD of triplicate independent sets of experiments.

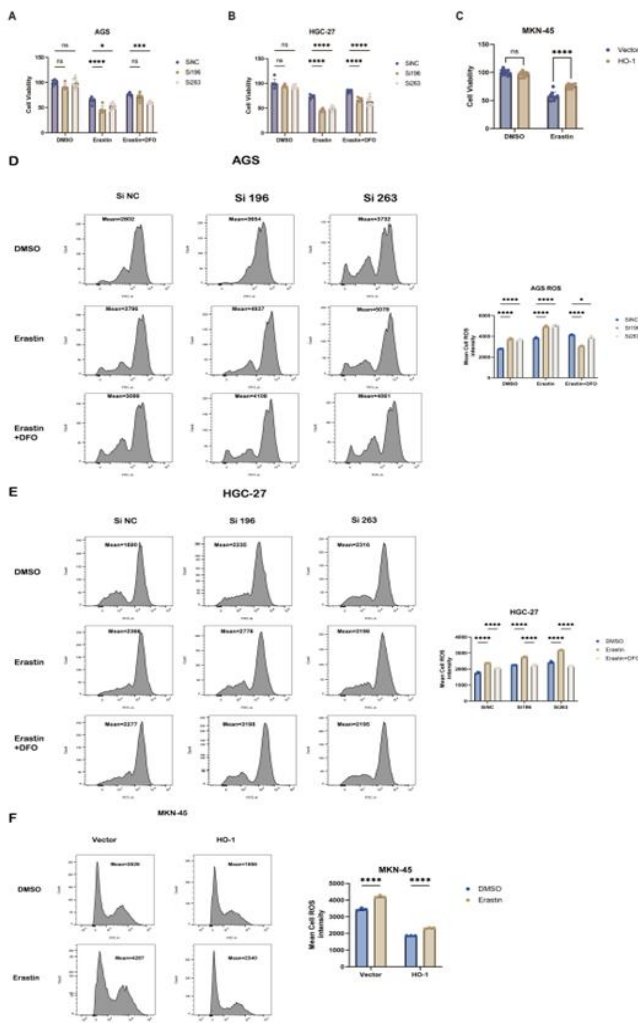
HO-1 reduces intracellular ROS and inhibits ferroptosis via GPX4

Knowing that HO-1 can regulate the GPX4 protein, and GPX4 is a key molecule in regulating ferroptosis, we investigated whether HO-1 affects the occurrence of ferroptosis through GPX4.

Treating AGS/HGC-27-siNC/AGS/HGC-27-si196-HO-1/AGS/HGC-27-si263-HO-1 cells with erastin (10 μ M) decreased the viability of cells more significantly than the DMSO-treated group. At the same time, the ferroptosis inhibitor deferoxamine(DFO 100uM) was used for the recovery experiment, and the results showed that the viability of AGS/HGC-27-si cells was increased(Figure 4: A, B).Moreover,treatment of MKN-45-Vector/ MKN-45-HO-1 cells with the ferroptosis inducer erastin (10 μ M) inhibited the decrease of HGC-27-HO-1 cell viability relative to the DMSO-treated group(Figure 4: C).These results suggest that HO-1 might be associated with Erastin-induced ferroptosis.

The level of ROS in MKN-45-Vector/MKN-45-HO-1 cells was further detected by flow cytometry. The results showed that in the erastin-treated group, HO-1 reduced the level of intracellular ROS (Fig. 4F).In AGS/HGC-27-siNC/AGS/HGC-27-si196-HO-1/AGS/HGC-27-si263-HO-1 cells, intracellular ROS was significantly increased after erastin treatment while ferroptosis inhibitor DFO rescued the above effect(Figure 4: D, E).

Figure 4: HO-1 reduces intracellular ROS and inhibits ferroptosis via GPX4.



A,B:Treating AGS/HGC-27-siNC/AGS/HGC-27-si196-HO-1/AGS/HGC-27-si263-HO-1cells with erastin(10 μ M) decreased the viability more significantly than the DMSO-treated group (***)(<math>***<0.0001</math>). After ferroptosis inhibitor DFO(100uM) treatment, the viability of AGS/HGC-27-si cells increased.

C :Treatment of MKN-45-Vector/MKN-45-HO-1 with the ferroptosis inducer erastin (10 μ M) inhibited the decrease of MKN-45-HO-1 cell viability relative to the DMSO-treated group (***)(<math>***<0.0001</math>)

D, E :The level of ROS in AGS/HGC-27-siNC/AGS/HGC-27-si196-HO-1/AGS/HGC-27-si263-HO-1 cells detected by flow cytometry. The results showed that AGS/HGC-27-si intracellular ROS was significantly increased after erastin treatment , while ferroptosis inhibitor DFO(100uM) reversed this process(***)(<math>***<0.0001</math>).

F: The level of ROS in MKN-45-Vector/MKN-45-HO-1 cells detected by flow cytometry.The results showed that in the erastin-treated group, HO-1 reduced the level of intracellular ROS (***)(<math>***<0.0001</math>).

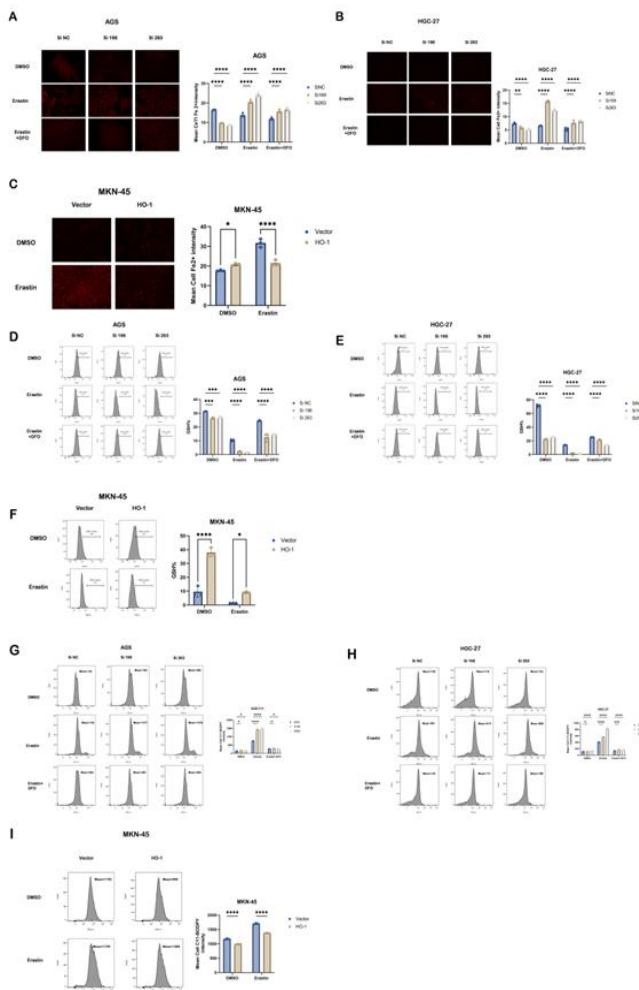
Furthermore, intracellular iron overload is one of the important signs of ferroptosis. Using FerroOrange to assess intracellular iron levels, we observed a significant decrease in sub-ferric ion content in HGC-27/AGS cells after HO-1 downregulation(Figure 5: A, B). However, treatment of AGS-si196- HO-1/ AGS-si263-HO-1 and HGC-27-si196-HO-1/ HGC-27-si263- HO-1 cells with Erastin (10 μ M) showed a more pronounced elevation of free ferrous ions in AGS/HGC-27-si cells, whereas DFO (100 μ M) inhibited the above effects (Figure 5: A, B). In contrast, the content of ferrous ions in MKN-45 cells increased with the upregulation of HO-1 expression (Figure 5: C).

Next, we analyzed the glutathione (GSH) levels, a crucial substrate of GPX4, and the lipid peroxidation product C11 BODIPY 581/591.

GSH content in HGC-27/AGS cells significantly decreased after HO-1 down-regulation, with a more pronounced effect after Erastin treatment, which was alleviated by DFO treatment (Figure 5: D, E). Conversely, GSH content in MKN-45 cells increased with the upregulation of HO-1 expression (Figure 5: F). Following HO-1 downregulation, C11 BODIPY 581/591 content significantly increased in HGC-27/AGS cells, with a more pronounced effect after Erastin treatment. This increase was attenuated by DFO treatment (Figure 5: G, H). In MKN-45 cells, HO-1 expression was upregulated and C11 BODIPY 581/591 content was downregulated, with a more significant effect after Erastin treatment (Figure 5: I).

The above experimental results confirmed that HO-1 could reduce intracellular ROS, and thus inhibit the occurrence of ferroptosis.

Figure 5: HO-1 inhibits lipid peroxidation in GC cells



A, B: Levels of ferrous ions (Fe²⁺) in HGC27/AGS-siNC / HGC27/AGS-si196-HO-1 / HGC27/AGS-si263-HO-1 cells treated with Erastin as well as DFO(100uM) were visualized by fluorescence microscopy. Data are shown as the mean ± SD of triplicate independent sets of experiments; statistical significance was assessed by paired t-test (* P < 0.05 , ** P < 0.01 , *** P < 0.001 , **** P < 0.0001). Representative images (left panel) and quantification results (right panel) are shown. The scale bar is: 100uM.

.C: In MKN-45-VECTOR/ MKN-45-HO-1 cells, HO-1 decreased the intracellular level of free ferrous iron. Representative images (left panel) and quantification results (right panel) are shown. The scale bar is: 100uM.

D, E: GSH content in HGC27/AGS-si cells decreased, and the difference was more significant after erastin treatment and increased after DFO (100uM) treatment (***<0.0001).

F: In MKN-45-VECTOR/ MKN-45-HO-1 cells, HO-1 increased intracellular GSH levels.

G, H: It was further observed by flow cytometry that knock down of HO-1 significantly increased intracellular lipid peroxidation and was antagonized by DFO (100uM) after treatment with Erastin.

I: Overexpression of HO-1, on the other hand, decreased MKN-45 cells' lipid peroxidation levels.

DISCUSSION

In the present study, we identified HO-1 as a regulatory factor promoting gastric cancer progression. Mechanistically, HO-1 inhibits ferroptosis by upregulating the transcription of GPX4, leading to increased GPX4 protein levels and decreased ROS in gastric cancer cells. This discovery not only sheds light on a novel aspect of gastric cancer progression but also offers a potential therapeutic target for its treatment.

Growing evidence supports the notion that HO-1 plays a role in accelerating tumor progression. Overexpression of HO-1 inhibits apoptosis induced by rapamycin and sorafenib Chatterjee et al. (2020). Moreover, articles about HO-1 and malignant progression of gastric cancer have been published in recent years. Studies have reported that CO produced by HO-1 metabolism has anti-inflammatory and anti-apoptotic effects Sun et al. (2016). Meanwhile, a research team found that HO-1 was highly expressed in gastric cancer tissues and correlated with poor prognosis of patients, and indicated that high expression of HO-1 inhibited the proliferation and invasion of gastric cancer cells (MKN-28, SGC-7901) Krukowska et al. (2022). Even, one team showed that HO-1 was observed in gastric cancer tissues in association with CD8-positive T-cell infiltration Ren et al. (2017). However, information regarding the relationship between HO-1 and the malignant progression of gastric cancer, particularly the mechanism involving ferroptosis, remains scarce. The present study is the first to elucidate that HO-1 can influence the malignant progression of gastric cancer through its association with ferroptosis.

Assessment of HO-1 expression levels in matched GC and non-GC tissues by gastric cancer public database data and immunohistochemical staining of gastric cancer tissues and paracancerous tissues, we observed that HO-1 was highly expressed in gastric cancer tissues. In addition, RT-qPCR and protein blotting assays confirmed elevated HO-1 expression in gastric cancer cell lines compared to normal gastric mucosa cells. However, CCK-8 and EDU in vitro proliferation assays showed that altering HO-1 alone had no impact on gastric cancer cell proliferation. While our clinical cases were relatively limited, prognostic information is undergoing further statistical analysis.

To further explore the relationship between HO-1 and gastric cancer, we explored whether HO-1 could influence gastric cancer progression through the medium of ferroptosis. Data analysis from public databases supported a connection between HO-1 and ferroptosis. Further experiments, including RT-qPCR and protein blotting, revealed consistent changes in GPX4 mRNA and protein expressions following HO-1 up or downregulation. This suggests that HO-1 may stabilize GPX4 protein levels through post-transcriptional translation. Notably, similar regulation by HO-1 was found to protect hepatocytes from ferroptosis Yin et al. (2012). In addition, this regulation demonstrated protective effects on renal tubular epithelial cells in a mouse model of cisplatin-induced acute kidney injury Yang et al. (2022). In summary, our findings establish a positive regulatory relationship between HO-1 and GPX4, the pivotal protein in ferroptosis. However, since HO-1 is not a transcription factor, the mechanism through which it affects the transcription process of GPX4 warrants further exploration.

Subsequent experiments revealed that knocking down HO-1 increased the sensitivity of gastric cancer cells to Erastin and elevated intracellular ROS levels.

In the context of cancer development, stimuli in the tumor microenvironment, including cytokine and growth factor release and metabolic remodeling, are crucial in addition to genetic changes. During metabolic remodeling, ROS plays a pivotal role as signaling molecules Lin et al. (2023). While essential for normal cell proliferation, excessive ROS can lead to cell death Hayes et al. (2020). This study demonstrates that HO-1 reduces intracellular ROS by stabilizing GPX4 protein expression, thereby maintaining ROS homeostasis in gastric cancer cells and inhibiting ferroptosis. This, in turn, contributes to the promotion of gastric cancer progression.

In summary, HO-1 expression increases during the malignant process of gastric cancer. Through the upregulation of GPX4 mRNA, it facilitates protein translation, resulting in reduced intracellular ROS and cellular protection from ferroptosis.

DECLARATIONS

Acknowledgements

This work was supported by the (Major Science and Technology Demonstration of Wuxi Science and Technology Bureau (No. WX18IVJN017)); (Top Medical Expert Team of 2021 Taihu Talent Plan Project, Medical Innovation Team of Wuxi (No. CXTD2021001)); (Cohort and Clinical Research Program of Wuxi Medical Center, Nanjing Medical University (No. WMCC202313)); (Major Program of Wuxi Medical Center, Nanjing Medical University

(No. WMCM202308)). We thank Bullet Edits Limited for the linguistic editing and proofreading of the manuscript.

Author Contributions Statement

Shiqi Shi: Conceptualization, Methodology, Formal Analysis, Writing - Original Draft;

Hanyu Wang, Huiyao Li, Xiaolu Yu: Data Curation, Writing - Original Draft, Writing - Review & Editing;

Xiaoli Wang: Visualization;

Chenjie Shen, Cenzhu Wang, Xi Wu, Shuai Liang, Tongxin Zhang, Rendu Wu: Resources, Supervision; Software, Validation

Dong Hua (Corresponding Author):

Conceptualization, Funding Acquisition, Resources, Supervision, Writing - Review & Editing.

Declaration of Interest

All authors disclosed no relevant relationships

Highlights

- 1.Heme Oxygenase-1 (HO-1) inhibits ferroptosis and promotes the progression of gastric cancer
- 2.Upregulation of HO-1 is expected to be a new therapeutic target in primary gastric cancer ;
- 3.HO-1 reduces intracellular ROS and inhibits ferroptosis via GPX4

REFERENCES

- 1.Sung H, Ferlay J, Siegel RL, et al. 2021 May. Global Cancer Statistics 2020: GLOBOCAN Estimates of Incidence and Mortality Worldwide for 36 Cancers in 185 Countries. *CA Cancer J Clin.* 71(3):209-249.
- 2.Cristescu R, Lee J, Nebozhyn M, et al. 2015 May. Molecular analysis of gastric cancer identifies subtypes associated with distinct clinical outcomes. *Nat Med.*21(5):449-56.
- 3.Dixon SJ, Lemberg KM, Lamprecht MR, et al. 2012 May 25. Ferroptosis: an iron-dependent form of nonapoptotic cell death. *Cell.*149(5):1060-72.
- 4.Alam J, Cook JL. 2007 Feb.How many transcription factors does it take to turn on the heme oxygenase-1 gene? *Am J Respir Cell Mol Biol.*36(2):166-174.
- 5.Frazer DM, Anderson GJ. 2014 Mar-Apr. The regulation of iron transport. *Biofactors.*40(2):206-14.

6. Bogdan AR, Miyazawa M, Hashimoto K, et al. 2016 Mar. Regulators of Iron Homeostasis: New Players in Metabolism, Cell Death, and Disease. *Trends Biochem Sci.*41(3):274-286.
7. Gao M, Monian P, Quadri N, et al. 2015 Jul 16. Glutaminolysis and Transferrin Regulate Ferroptosis. *Mol Cell.* 59(2):298-308.
8. Sun X, Ou Z, Xie M, et al. 2015 Nov 5. HSPB1 as a novel regulator of ferroptotic cancer cell death. *Oncogene.*34(45):5617-25.
9. Wang Y, Zheng L, Shang W, et al. 2022 Nov. Wnt/beta-catenin signaling confers ferroptosis resistance by targeting GPX4 in gastric cancer. *Cell Death Differ.* 29(11):2190-2202.
10. Zhang H, Deng T, Liu R, et al. 2020 Feb 27. CAF secreted miR-522 suppresses ferroptosis and promotes acquired chemo-resistance in gastric cancer. *Mol Cancer.* 19(1):43.
11. Ryter SW, Alam J, Choi AM. 2006 Apr. Heme oxygenase-1/carbon monoxide: From basic science to therapeutic applications. *Physiol Rev.*86:583–650.
12. Vitek L, Schwertner HA. 2007. The heme catabolic pathway and its protective effects on oxidative stress-mediated diseases. *Adv Clin Chem.*43:1–57.
13. Kwon MY, Park E, Lee SJ, et al. 2015 Sep 15. Heme oxygenase-1 accelerates Erastin induced Ferroptotic cell death. *Oncotarget.* 6:24393–24403.
14. Chang LC, Chiang SK, Chen SE, et al. 2018 Mar. Heme oxygenase-1 mediates BAY 11-7085 induced ferroptosis. *Cancer Lett.* 416:124–137.
15. Hassannia B, Wiernicki B, Ingold I, et al. 2018 Aug 1. Nano-targeted induction of dual ferroptotic mechanisms eradicates high-risk neuroblastoma. *J Clin Invest* 128:3341–3355.
16. Sugimoto R, Tanaka Y, Noda K, et al. 2012 Dec. Preservation solution supplemented with biliverdin prevents lung cold ischaemia/reperfusion injury. *Eur J Cardiothorac Surg.* 42(6):1035-41.
17. Jomova K, Vondrakova D, Lawson M, et al. 2010 Dec. Metals, oxidative stress and neurodegenerative disorders. *Mol Cell Biochem.* 345:91–104.
18. Sunamura M, Duda DG, Ghattas MH, et al. 2003. Heme oxygenase-1 accelerates tumor angiogenesis of human pancreatic cancer. *Angiogenesis.*6:15–24.
19. Deshane J, Chen S, Caballero S, et al. 2007 Mar 19. Stromal cell-derived factor 1 promotes angiogenesis via a heme oxygenase 1-dependent mechanism. *J Exp Med.* 204:605–618.
20. Luo P, Liu D, Zhang Q, et al. 2022 May. Celastrol induces ferroptosis in activated HSCs to ameliorate hepatic fibrosis via targeting peroxiredoxins and HO-1. *Acta Pharm Sin B.* 12(5):2300-2314.
21. Tang Z, Ju Y, Dai X, et al. 2021 Jul. HO-1-mediated ferroptosis as a target for protection against retinal pigment epithelium degeneration. *Redox Biol.*43:101971.
22. Huang Y, Yang Y, Xu Y, et al. 2021 Apr 12. Nrf2/HO-1 Axis Regulates the Angiogenesis of Gastric Cancer via Targeting VEGF. *Cancer Manag Res.* 13:3155-3169.
23. Yin Y, Liu Q, Wang B, et al. 2012 Apr. Expression and function of heme oxygenase-1 in human gastric cancer. *Exp Biol Med (Maywood).* 237(4):362-71.
24. Yang W, Wang Y, Zhang C, et al. 2022 Apr 4. Maresin1 Protect Against Ferroptosis-Induced Liver Injury Through ROS Inhibition and Nrf2/HO-1/GPX4 Activation. *Front Pharmacol.* 13:865689.
25. Lin Q, Li S, Jin H, et al. 2023 Feb 13. Mitophagy alleviates cisplatin-induced renal tubular epithelial cell ferroptosis through ROS/HO-1/GPX4 axis. *Int J Biol Sci.* 19(4):1192-1210.
26. Hayes JD, Dinkova-Kostova AT, Tew KD. 2020 Aug 10. Oxidative stress in cancer. *Cancer Cell.* 38:167–97.
27. Chatterjee R, Chatterjee J. 2020 Apr. ROS and oncogenesis with special reference to EMT and stemness. *Eur J Cell Biol.*99:151073.
28. Sun X, Ou Z, Chen R, et al. 2016 Jan. Activation of the p62-Keap1-NRF2 pathway protects against ferroptosis in hepatocellular carcinoma cells. *Hepatology.* 63(1):173-84.
29. Krukowska K, Magierowski M. 2022 Jul. Carbon monoxide (CO)/heme oxygenase (HO)-1 in gastrointestinal tumors pathophysiology and pharmacology - possible anti- and pro-cancer activities. *Biochem Pharmacol.* 201:115058.
30. Ren QG, Yang SL, Li PD, et al. 2017 Nov. Low heme oxygenase-1 expression promotes gastric cancer cell apoptosis, inhibits proliferation and invasion, and correlates with increased overall survival in gastric cancer patients. *Oncol Rep.* 38(5):2852-2858.
31. Yin Y, Liu Q, Wang B, et al. 2012 Apr. Expression and function of heme oxygenase-1 in human gastric cancer. *Exp Biol Med (Maywood).* 237(4):362-71.
32. Kwon MY, Park E, Lee SJ, et al. 2015 Sep 15. Heme oxygenase-1 accelerates Erastin induced Ferroptotic cell death. *Oncotarget.* 6:24393–24403.

33.Chang LC, Chiang SK, Chen SE, et al. 2018 Mar 1. Heme oxygenase-1 mediates BAY 11-7085 induced ferroptosis. *Cancer Lett.*416:124–137.

34.Song X, Long D. 2020 Apr 21. Nrf2 and Ferroptosis: A New Research Direction for Neurodegenerative Diseases. *Front Neurosci.*14:267.

35.Dang R, Wang M, Li X, et al. 2022 Feb 7. Edaravone ameliorates depressive and anxiety-like behaviors via Sirt1/Nrf2/HO-1/Gpx4 pathway. *J Neuroinflammation.* 19(1):41.

36.Li D, Wang Y, Dong C, et al. 2023 Jan.CST1 inhibits ferroptosis and promotes gastric cancer metastasis by regulating GPX4 protein stability via OTUB1. *Oncogene.* 42(2):83-98.